2.36 SATELLITE-DERIVED LAND SURFACE EMISSIVITY FOR ARM AND CERES

William L. Smith Jr.
Analytical Services and Materials, Inc., Hampton, VA

Patrick Minnis, David F. Young
Atmospheric Sciences, NASA Langley Research Center, Hampton, VA

Yan Chen
Science Applications International Corporation, Hampton, Virginia

1. Introduction

Surface emissivity, an important parameter for many remote sensing applications, is difficult to determine because it requires an accurate specification of the surface skin temperature. Because of the difficulty in determining skin temperature without knowing emissivity first, many applications rely on limited laboratory estimates of the emissivity of pure surfaces. These generally do not adequately simulate the Earth's natural surfaces as seen from a satellite imager in space. In this paper, we present a new technique to derive surface emissivity from clear-sky, multispectral satellite data for three infrared channels (3.9 or 3.7, 10.8 and 12.0 μm) common to many of today's meteorological satellites. The technique is iterative and relies on the assumption of a constant ratio of 3.9-to-10.8 μm emissivity for a given region. The ratio is measured at night. By utilizing daytime data to exploit a second term in a simplified form of the radiative energy equation at the surface for 3.9 μm, we estimate the true 3.9-μm emittance. The true skin temperature may then be calculated and applied to derive the surface emissivity at 10.8 and 12.0 μm. Atmospheric effects are accounted for using correlated k-distribution functions for the 3 channels and atmospheric temperature and moisture profiles from radiosondes and numerical weather prediction models. The technique is applied to half-hourly Geostationary Operational Environmental Satellite (GOES) data in a domain encompassing the Atmospheric Radiation Measurement Program (ARM) Southern Great Plains (SGP) domain of the United States and globally using NOAA-9 Advanced Very High Resolution Radiometer data from the International Satellite Cloud Climatology Project for the Clouds and Earth's Radiant Energy System (CERES) experiment. The results show a significant dependence on season and surface type and are valuable for improving surface skin temperature estimates. Improved surface emissivity specification should also improve the accuracy of satellite-derived infrared semi-transparent cloud properties.

*Corresponding author address: William L. Smith, Jr., AS&M, Inc., Hampton, VA 23666,
email: w.l.smith@larc.nasa.gov.

2. Data

Solar-infrared (SI, 3.9 μm), infrared (IR, 10.8 μm), and split-window (WS, 11.9 μm) data taken at a nominal 4-km resolution from the GOES-8 imager were averaged on a 0.5° equal angle grid between 32°N and 42°N and between 90°W and 104°W on a half-hourly basis for all grid boxes that were classified as completely clear. This grid is roughly centered on the SGP Central Facility (SCF) at 36.48°N, 97.59°W. Within the domain, the satellite viewing zenith angle θ ranges from 38° in the southeastern corner to 60° in the northeastern corner. At the SCF, $\theta \approx 52°$. The dataset includes April 9 – May 9, 1996 (April); June 18 – July 18 (July) and September 15 – October 5, 1997 (September); and January 1 – 31, 1998 (January) to represent the four seasons. Clear regions were determined using the approach of Minnis et al. (1995). The grid-box averaging is performed using pixel radiances. The mean radiance is converted to an equivalent blackbody temperature T_i. Here, *i* corresponds to a channel number: 2 for SI, 4 for IR, and 5 for WS.

Derivation of the surface emitted radiances requires correcting the observed satellite radiances for the attenuation by atmospheric

gases. Water vapor is the primary absorber at these wavelengths. Atmospheric profiles of temperature and humidity were developed for each image from the 60-km resolution, 3-hourly, 60-km resolution Rapid Update Cycle analyses (Benjamin et al., 1994) by linear interpolation.

2. Methodology

The radiance exiting the surface for a given channel, i, is

$$B_i(T_{si}) = \varepsilon_i\,(\mu)\,B_i(T_{skin}) + (1-\varepsilon_i)L_{ai}, \qquad (1)$$

where B is the Planck function, ε is the surface emissivity, $\mu = \cos\theta$, L_a is the downwelling atmospheric radiance at the surface, T_{skin} is the skin temperature and T_{si} is the apparent radiating temperature at the surface. The observed radiance at the top of the atmosphere (TOA) is due to a combination of radiances from the surface and atmosphere. In a simple form,

$$B_i(T_i) = \varepsilon_{ai}\,B_i(T_{ai}) + (1-\varepsilon_{ai})\,B_i(T_{si}), \qquad (2)$$

where ε_a and T_a are the effective emissivity and effective temperature of the atmosphere, respectively. Thus, T_{si} can be derived by solving (2), given the observed radiance, the temperature and humidity profiles, and a means for converting the atmospheric gas concentrations to spectral optical depth. The latter was accomplished using the correlated-*k* method of Kratz (1995) for the GOES imager channels. The actual solution to (2) is found by computing the emission and absorption for each of 37 atmospheric layers using the correlated-*k* optical depth of the layer. Sequential removal of the contribution and absorption of each layer from the observed radiance down to the surface yields T_{si}. Rearranging (1) yields

$$T_{skin} = B_i^{-1}\{([B_i(T_{si}) - L_{ai}] / \varepsilon_i) + L_{ai}\} \qquad (3)$$

for any time of day. If the reflected component is assumed to be negligible, then for channel 4, (3) reduces to

$$T_{skin} = B_4^{-1}\{B_4(T_{s4}) / \varepsilon_4\}. \qquad (3a)$$

Similarly,

$$\varepsilon_2 = B_2(T_{s2}) / B_2(T_{skin}). \qquad (4)$$

Using the atmospheric corrections for each channel to obtain the apparent surface temperatures in each channel, it is possible to define the apparent SI emissivity as

$$\varepsilon_2' = B_2(T_{s2}) / B_2(T_{s4}), \qquad (5)$$

a value that can be easily computed at night from the observations. During the daytime, solar radiation is reflected from the surface in channel 2. Figure 1 shows the observed TOA temperature difference $\Delta T_{24} = T_2 - T_4$ during a clear sky day on October 1, 1997. The difference is nearly constant at ~ 2K during the night but variable during the day due to the reflection of solar radiation. Although the maximum T_4 occurs near local noon (1800 UTC), ΔT_{24} peaks earlier at 1645 UTC when the relative azimuth angle φ is a maximum. In general, ΔT_{24} is asymmetrical around local noon suggesting that the reflected

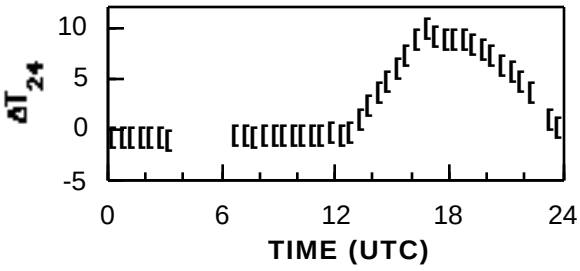

Fig. 1. GOES-8 brightness temperature difference (3.9 μm minus 10.8 μm) for the clear sky day of October 1, 1997 over the ARM SGP Central Facility.

component in channel 2 is not isotropic. Thus, some means for correcting for the anisotropy may be needed to minimize errors in the derived emissivities. The surface reflectance is

$$\rho_2 = \chi(\mu_0,\mu,\varphi)\,\alpha_2(\mu_o), \qquad (6)$$

where $\chi(\mu_0,\mu,\varphi)$ is the anisotropic correction factor, $\mu_0 = \cos(\theta_o)$, φ is the relative azimuth angle, and α is the surface albedo. Thus, the apparent surface temperature in channel 2 is

$$B_2(T_{s2}) = \varepsilon_2\{B_2(T_{skin})\} + \alpha_2\,\chi S_2', \qquad (7)$$

where the solar radiance reaching the surface S_2' is the channel-2 solar constant adjusted for the Earth-sun distance and solar zenith angle and attenuated by atmospheric absorption as the incoming radiance traverses the atmosphere to the

surface. The attenuation is computed as in (2), except in reverse order starting with the incoming solar radiance. Neglecting any solar-zenith angle dependence of the surface albedo and invoking Kirchoff's law ,

$$\alpha_2 = (1 - \varepsilon_2). \qquad (8)$$

If it is assumed that the apparent emissivity is constant, then by rearranging (4), (5), and (8) and substituting into (7), the channel-2 radiance exiting the surface for radiation incident at μ_o is

$$B_2(T_{s2}) = \varepsilon_2'\{B_2(T_{s4})\} + (1 - \varepsilon_2)\,\delta(\mu_o)\chi S_2', \qquad (9)$$

where the directional albedo normalization factor, $\delta(\mu_o) = \alpha(\mu_o)/\alpha(\mu_o = 0°)$, is assumed to be unity. The observed channel-2 radiance is corrected for attenuation to obtain $B_2(T_{s2})$ using (2) as described earlier. By deriving an average value of ε_2' from nighttime clear data, the true surface emissivity ε_2 is determined from (9) using daytime data . The skin temperature can then be computed from (4) and the emissivity in any channel is found using (1).

The key parameter, ε_2', is assumed to be constant over a wide range of temperatures for a given surface. To test this assumption, ε_2' was computed for T_{skin} between 240 and 325K using $\varepsilon_2 = 0.700 - 0.995$ and $\varepsilon_4 = 0.750 - 0.998$ yielding $\varepsilon_2' = 0.700 - 0.997$. For a given set of emissivity pairs, the maximum variation of ε_2' over the full range of temperatures is 0.4%. For an extreme diurnal cycle of 50°C, the maximum range of ε_2' is 0.2%. Nearly all values of ε_2' are constant to within $\pm$ 0.1% of the value computed at the mid temperature range. Simulated retrievals of ε_2, ε_4, and ε_5 using a computed value of ε_2' for a specified surface are accurate to better than $\pm$0.1%. Thus, if the instrument calibrations and anisotropic corrections are flawless, zenith angle dependencies are negligible, the atmospheric attenuation is correctly determined, the reflected component in (1) is negligible and the surface characteristics are temporally invariant, this technique should produce an extremely accurate value of emissivity for a given location.

3. Results

Minnis et al. (1998) employed the above technique to compute grid box averaged values of ε_2', ε_2 , ε_4 and ε_5. A radiance equivalent to a blackbody temperature of 344.8 K was used for the channel-2 solar constant. Due to a lack of knowledge of the bidirectional reflectance patterns at 3.9 μm, the visible-channel bidirectional reflectance model described by Minnis and Harrison (1984) was used for χ. This will likely induce some level of error in the derived emissivities. To examine this potential effect, hourly averaged daytime SI emissivities were computed over the SCF and plotted in figures 2 for the April and July. The emissivities are also plotted assuming a Lambertian surface (χ=1). $\varepsilon_2(t)$ is relatively flat for the cases using the visible BRDF's compared to those computed using a Lambertian surface. In fact, the Lambertian assumption yields an increase in the range of $\varepsilon_2(t)$ of over 300% for April to about 0.05. For July, the BRDF has a minimal impact, apparently because the values of χ are close to unity for most time slots. During September and January (not shown), the ranges double from 0.04 to 0.08 and 0.02 to 0.04, respectively. The Lambertian assumption for the channel-3 reflectance causes similar changes in the channel-4 and –5 emissivities. If it is assumed that emissivity is constant during the daytime, then it may be concluded that correction for the anisotropic reflectance is important in the derivation of surface emissivity from the day-night datasets. While not perfect, the visible-channel BRDF factors used here reduce the variability by a factor of 2, on average, indicating the corrections are of the proper sign.

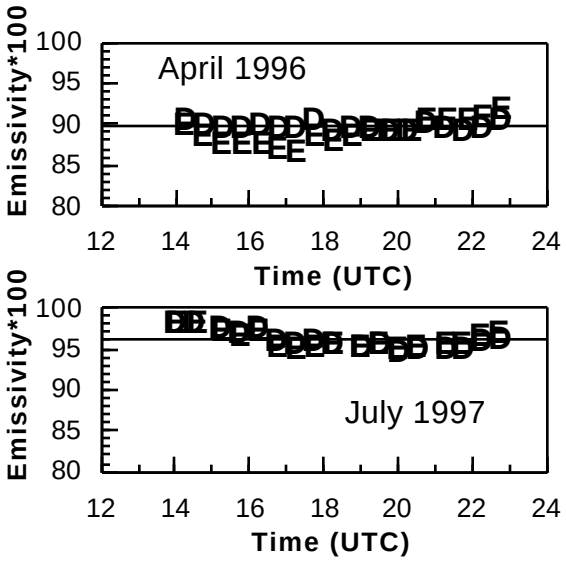

Fig. 2. Monthly hourly averaged emissivities over the ARM SCF derived with a Lambertian assumption (circles) and using visible channel BRDF's (crosses).

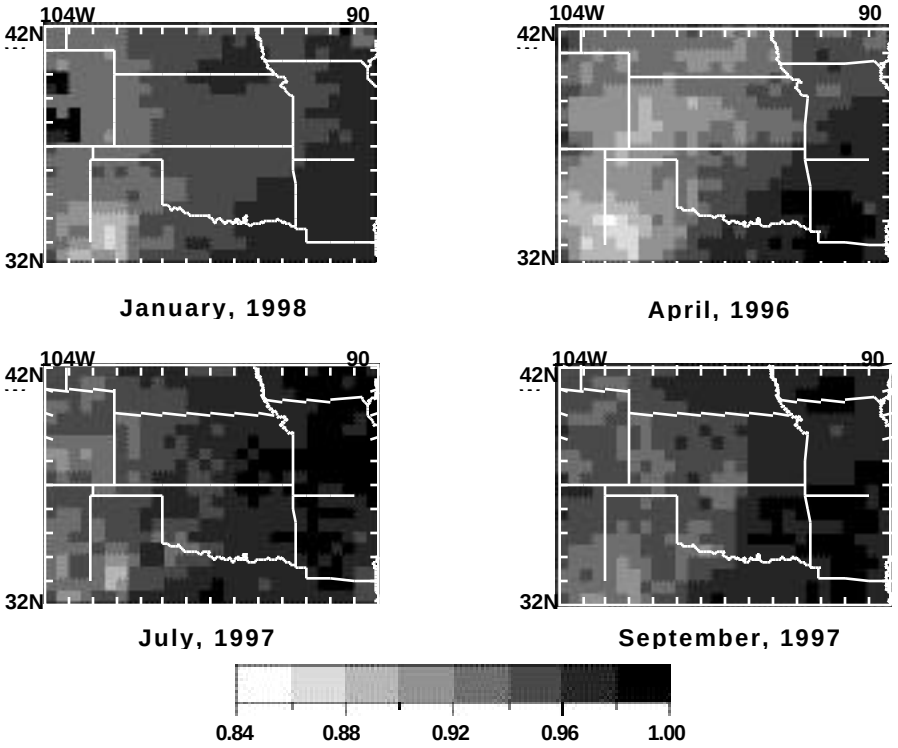

Fig. 3. Daytime 3.9-μm surface emissivity from GOES-8 data.

Figure 3 shows the mean channel-2 emissivities derived from daytime data. In general, ε_2 ranges from 0.8 to 0.99 decreasing from east to west. The emissivities appear to be well-correlated with vegetation type: forested areas having values around 0.96-0.99, drier grasslands with values around 0.89, and croplands around 0.95. The seasonal cycle appears to follow the greening of the local vegetation. The spatial and seasonal patterns are similar for ε_4 and ε_5 although the magnitudes are somewhat larger. Generally, ε_4 and ε_5 range from 0.97 to 1.01 and 0.95 to 1.02, respectively. The values greater than unity were more common when the atmospheric water vapor loading was high. Also, the WS emissivities were considerably noisier than the SI and IR emissivities owing to the increased sensitivity of the 11.9 μm channel to atmospheric humidity. It appears that neglecting the reflected downwelling component in (1) may lead to an overestimate in the emissivity retrievals. The computations formulated above will be performed again, both for the SGP and globally using the ISCCP NOAA-9 dataset, this time including the reflected downwelling component. These new results will be presented at the conference.

References

Benjamin, S. G., K. J. Brundage, and L. L. Morone, 1994: The Rapid Update Cycle. Part I: Analysis/model description. Technical Procedures Bulletin No. 416, NOAA/NWS, 16 pp. [Available from National Weather Service, Office of Meteorology, 1325 East-West Highway, Silver Spring, MD 20910]

Kratz, D. P., 1995: The correlated *k*-distribution technique as applied to the AVHRR channels. *J. Quant. Spectrosc. Rad. Transf.*, **53**, 501-507.

Minnis, P. and E. F. Harrison, 1984: Diurnal variability of regional cloud and clear-sky radiative parameters derived from GOES data; Part III: November 1978 radiative parameters. *J. Climate Appl. Meteorol.*, **23**, 1032-1052.

Minnis, P. D. F. Young and W. L. Smith, Jr., 1998: Surface Emissivity Derived From Multispectral Satellite Data: *Proceedings of the Eighth Atmospheric Radiation Measurement Program Science Team Meeting*, 489-494.